Nature Environment and Pollution Technology
An International Quarterly Scientific Journal

p-ISSN: 0972-6268
(Print copies up to 2016)
e-ISSN: 2395-3454

Vol. 21 | No. 3 | pp. 1463-1470 | 2022

Original Research Paper

https://doi.org/10.46488/NEPT.2022.v21i03.056

Open Access Journal

Strength Characteristics of Cement-Modified Iron Tailings and Their Adsorption on Graphene Oxide

Ping Jiang*(**)†, Xuhui Zhou, Jiandong Yang** and Lin Zhou****

*School of Transportation, Southeast University, Nanjing, Jiangsu 211189, China

**School of Civil Engineering, Shaoxing University, Shaoxing, Zhejiang 312000, China

†Corresponding author: Ping Jiang; jiangping@usx.edu.cn

Nat. Env. & Poll. Tech.
Website: www.neptjournal.com

Received: 18-10-2021
Revised: 05-12-2021
Accepted: 23-12-2021

Key Words:
Cement-modified iron tailings
Graphene oxide
Mechanical properties
Adsorption characteristics
Micro mechanism

ABSTRACT

To explore the mechanical properties of cement-modified iron tailings (CIT) and its adsorption on graphene oxide (GO), the unconfined compressive strength (UCS) tests of CIT with 10% cement were carried out for 7 and 28 days. CIT adsorption of GO was carried out under the conditions of different pH, CIT dosage, and GO initial concentration. The micro characterization of CIT adsorption of GO was carried out by SEM, TEM, AFM, EDS, FT-IR, XRD, and XPS. The results show that: (1) the CIT strength of 28 d curing age is 1202 kPa is twice of 7 d. (2) At the same pH, the GO adsorption effect of CIT at 7 days curing age was better than that at 28 days. When pH is 6, CIT content is 50 mg, and GO initial concentration is 100 $mg.L^{-1}$, CIT has the best adsorption effect on the GO, and the removal rate reached 93.5%. (3) Through microscopic characterization, it can be concluded that the bound water in the CIT structure and the asymmetric stretching vibration of the O-H bond in hydrated calcium silicate (C-S-H) are the main factors affecting the adsorption of GO. The above research results show that CIT not only has good strength properties but also has good adsorption properties for GO. CIT is a potential environmental treatment material.

INTRODUCTION

Graphene is a new material that consists of carbon atoms stacked in a single hexagonal honeycomb, formed by an sp^2 hybrid connection. It is widely used in the research of various materials because it has been found that graphene has ultra-high- strength, good toughness, light transmittance, and excellent carrier mobility. With the continuous progress of production technology, a large number of wastes containing graphene derivatives will enter the soil, air, and water. Many studies show that graphene derivatives have an impact on the environment and biological toxicity. Guan et al. (2014) used MTT colorimetry to detect the effect of silk fibroin graphene oxide composite membrane on the relative proliferation rate (RGR) of mouse cells. The results showed that the concentration of graphene oxide (GO) increased and the cytotoxicity increased, but when the concentration of GO was lower than 1 wt%, there was no obvious cytotoxicity. Schinwald et al. (2016) and Qiao et al. (2013) have studied and proved the toxicity of GO to the human body. Graphene will deposit in alveoli when entering the human lungs. In addition, graphene also has genetic material toxicity and will seriously damage DNA (Jia 2019, Li et al. 2016, 2018).

Therefore, the effective treatment of toxic pollution of GO aqueous solution is an important research topic at present. At present, the main methods of sewage treatment include the adsorption method, ion exchange method, extraction method, and membrane analysis method (Liu & Wang 2003, Luo et al. 2019). The commonly used sewage treatment method is the adsorption method, which uses the porosity and other characteristics of the adsorbent to adsorb one or several pollutants in sewage, recover or remove these pollutants, to purify sewage (Zhao et al. 2015, Sun et al. 2017, Tang et al. 2016, Yoon et al. 2016). Luan and Tang (1993) measured that the specific surface area of tailings is 30 $m^2.g^{-1}$~40 $m^2.g^{-1}$. By comparing the performance of tailing sand in adsorbing Cu^{2+}, Pb^{2+}, and Cd^{2+}, the results show that tailing sand has a strong adsorption capacity for heavy metal ions, especially when the pH is above 5.

Finding an adsorbent material with high economic benefits has always been an important goal of water pollution control. In the world, the stock of metal tailings is very huge, of which iron tailings account for the vast majority (Bing et al. 2018). The resource application of iron tailings is an effective way to reduce the stock of tailings. Due to the single-particle size and low strength of iron tailings, it is difficult to be directly applied. It can be modified with cement to improve its mechanical properties. Therefore, this test first studies the strength characteristics of cement-modified iron tailings (CIT) and uses the CIT after hydration reaction to

adsorb GO aqueous solution to study the performance of cement iron tailings in removing GO from aqueous solution to achieve the purpose of sustainable development of ecological environment.

MATERIALS AND METHODS

Materials

Added 10% cement into iron tailings to obtain CIT samples. Conducted unconfined compressive strength test after curing for 7 and 28 days. Ground the tested CIT sample to powder state as adsorbent for adsorbing GO. The adsorbate was a GO aqueous solution, the manufacturer was Suzhou Tang Feng Technology Co., Ltd. in China, and its concentration was 2 mg.mL^{-1}. The adsorption test process under different acid-base environmental conditions was as follows: first sucked 3 mL GO solution with a pipette and put it into the reagent bottle, then added 47 mL deionized water with a resistivity of 18 MΩ• cm to the reagent bottle, adjust the pH value with NaOH and HCl solution with a concentration of 0.1 mol.L^{-1}, weighed the ground CIT with a high-precision electronic scale as the adsorbent, and then put the reagent bottle into the ultrasonic instrument for 30 min, Then put the oscillator into oscillation for 1 h, set the speed to 240 rpm and the temperature to 30°C, and finally put it into the incubator for 12 h. The incubator was set to 30°C, that is, T = 303 K.

Batch Experiments

The mechanical test mainly used the full-automatic unconfined compression tester of Nanjing TKA Co., Ltd. in China. Scanning electron microscopy (SEM, JSM-6360LV), energy-dispersive X-ray spectroscopy (EDX), transmission electron microscopy (TEM, JEM-2100F), atomic force microscopy (AFM, SPA400), X-ray diffractometer (XRD, Empyreal), X-ray photoelectron spectroscopy (XPS, Thermo ESCALAB 250xi) and Fourier infrared spectroscopy (FT-IR, Nexus) were mainly used for microscopic characterization. Among them, SEM, TEM, and AFM were used to characterize the micromorphology of the material, EDS was used to analyze the surface composition, XRD was used to analyze the phase of the adsorbed material, XPS was used to analyze the information of the element composition and content, chemical state, molecular structure and chemical bond of the compound, and FT-IR was used to determine the chemical composition of the adsorbed crystal through the absorption peak of the functional group of the infrared spectrum.

Sucked 1 mL supernatant of GO aqueous solution adsorbed by CIT after standing, transferred it into the test tube, added deionized water to the 25 mL scale mark, and then shook it evenly. The remaining GO concentration in the supernatant aqueous solution was analyzed by UV-Vis spectrophotometer at the wavelength of 210 nm. To ensure the test accuracy, each data was tested three times, and the relative error was within 5%. The following three formulas were used to calculate the removal rate R, adsorption capacity $Q_{e,}$ and distribution coefficient K_d.

$$R=\frac{C_0-C_e}{C_0}\times 100\% \quad \ldots(1)$$

$$Q_e=\frac{(C_0-C_e)\times V}{m} \quad \ldots(2)$$

$$K_d=\frac{Q_e}{C_e} \quad \ldots(3)$$

Where, C_0 is the initial concentration (mg.L^{-1}), C_e is the equilibrium concentration (mg.L^{-1}), V is the volume of GO aqueous solution (L), and m is the mass of adsorbent (mg).

RESULTS AND DISCUSSION

Mechanical Properties of CIT

The stress-strain curves of 7 d and 28 d CIT can be obtained through an unconfined compressive strength test, as shown in Fig. 1.

It can be seen from Fig. 1 that the stress-strain curve of CIT was a softening curve, that is, with the increase of strain, the stress first increases, reached the peak, and the stress gradually decreased with the increase of strain, and finally tended to be stable. From the curve, the unconfined compressive strength of CIT after curing for 7 d and 28 d was 614 kPa and 1202 kPa, respectively, indicating that adding cement to iron tailings can effectively improve its mechanical properties, and the strength of CIT increases by about twice when the curing age increases from 7 d to 28 d. This is because calcium silicate hydrate (C-S-H) gel produced by the hydration of cement can reinforce iron tailings. The

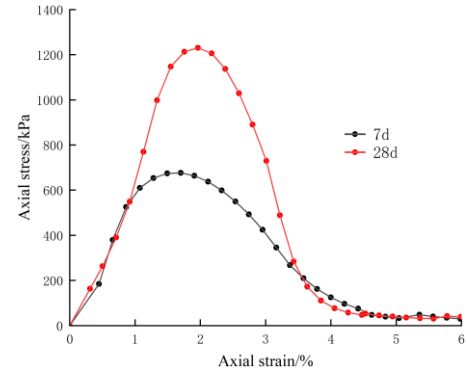

Fig. 1: CIT unconfined compressive strength.

cement hydration reaction in CIT for 7 d was not complete, resulting in less C-S-H, which cannot fully reinforce the iron tailings. However, the cement hydration reaction continued after 7 days, and it is not completed until 28 days, resulting in more C-S-H and a better reinforcement effect on iron tailings, which was reflected in the increase of unconfined compressive strength. By testing the zeta potential of CIT at 7 d and 28 d, the potential was - 16 mv and - 10 mv, respectively, indicating that the bound water in CIT decreased and the microstructure was more stable from 7 d to 28 d.

Adsorption Performance OF CIT ON GO

Effect of pH on GO adsorption: Firstly, the performance of GO aqueous solution adsorbed by 7 d CIT and 28 d CIT was compared, and the pH was set as 3, 7, and 10. Fig. 2 shows the adsorption capacity, adsorption rate, and partition coefficient of GO removed by CIT at 7 and 28 days. Both have the most obvious adsorption effect at pH 7, and the adsorption effect of 7 d CIT is better than that of 28 d CIT. The main reason may be that, on the one hand, the cement hydration reaction in 7 d CIT has not been completely completed. Due to its large surface area and a large number of epoxy functional groups on the lamella, GO will form a recombinant flocculation structure in the unreacted CIT, resulting in a low GO content in the supernatant (Wang 2017). On the other hand, the hydration reaction of CIT after 28 d is complete. The hydrated calcium silicate (C-S-H) gel produced by cement hydration completely solidified the iron tailings, resulting in the reduction of the iron tailings contacting with GO solution, resulting in the weakening of its adsorption effect on GO. At the same time, this phenomenon is also reflected in the change of solution after adsorption. It can also be seen from the comparison of (a) and (b) in Fig. 3 that the supernatant after CIT adsorption for 7 days is relatively clear.

To further study the adsorption effect of CIT on GO at the curing age of 7 days, the adsorption effect of CIT at different pH (3-10) was discussed. The CIT content was controlled to 50 mg. Fig. 4 shows the adsorption capacity, adsorption rate, and distribution coefficient of CIT on GO at different pH.

It can be seen from Fig. 4 that the adsorption capacity Q_e and removal rate R of GO removed by CIT first increase slowly with the increase of pH value, and then decrease rapidly when pH is 8, indicating that it is not conducive to CIT to adsorb GO in aqueous solution in an alkaline environment. It can be seen from the partition coefficient K_d that the adsorption effect is the best when pH is 6. At this time, the adsorption capacity Q_e is 114.9 mg.g^{-1}, the removal rate R is 95.8%, and the partition coefficient K_d is 22.6, The corresponding solution test picture after adsorption is shown in Fig. 5, which is completely consistent with the trend of the test data. The clarity of the solution is obviously layered in the acidic environment, there are more and more clear aqueous solutions in the upper part, and the clarity of the solution gradually becomes better, which indicates that the adsorption effect of CIT is better. However, in an alkaline environment, the solution after CIT adsorbs GO becomes more and more turbid, there is no obvious stratification, and the upper aqueous solution is less and less, which indicates that CIT adsorbs GO better in an acidic environment.

Effect of CIT content on GO adsorption: Fig. 6 shows the adsorption capacity, adsorption rate, and distribution coefficient of GO under different CIT contents. Among them, pH = 6, C_0 = 120 mg.L^{-1}, equilibrium time is 12 h, T = 303 K, CIT is 30 mg, 40 mg, 50 mg, 60 mg and 70 mg.

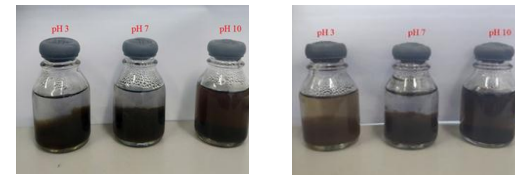

(a) CIT with 7d curing time (b) CIT with 28d curing time

Fig. 3: Adsorption effect at different ages.

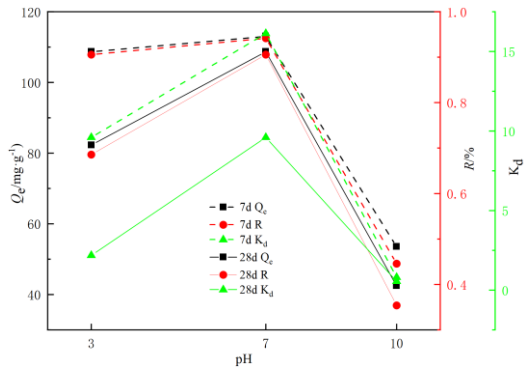

Fig. 2: Effect of pH on GO adsorption by CIT at different ages.

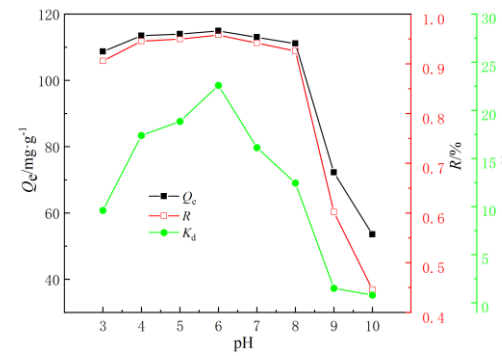

Fig. 4: Effect of pH on GO adsorption by CIT at 7-day.

It can be seen from Fig. 6 that with the increase of CIT content, the adsorption capacity of CIT on GO continues to decrease, which is due to the decrease of steric hindrance and increase of molecular weight when CIT is excessive, and the adsorption capacity of GO on the surface of CIT particles decreases (Yi et al. 2012). However, the adsorption rate and partition coefficient of GO increased with the increase of CIT content, reaching the maximum when CIT content is 50 mg. When CIT continues to increase, the adsorption rate and partition coefficient will decrease with the adsorption capacity. This shows that we should reasonably select high adsorption capacity (low adsorbent consumption) or high adsorption rate according to the actual situation. In this study, 50 mg CIT was used for the follow-up test. The solution image after adsorption also shows this law, as shown in Fig. 7. The solution is the most turbid when CIT is 30 mg, and the upper separator is the clearest when CIT is 50 mg.

Effect of initial concentration of GO on GO adsorption: When the initial concentrations of GO were 80 mg.L^{-1}, 100 mg.L^{-1}, 120 mg.L^{-1}, 140 mg.L^{-1}, and 160 mg.L^{-1}, CIT had a better adsorption effect on GO. Fig. 8 shows that the adsorption capacity is affected by the initial concentration of GO.

It can be clearly seen from Fig. 8 that with the increase of GO concentration, the adsorption capacity of CIT to GO gradually increases, but the adsorption rate R and partition coefficient K_d increase first and then decreases with the increase of the initial concentration of GO. When the initial concentration is 100 mg.L^{-1}, it reaches the maximum value, which is R=93.5% K_d=14.3. This shows that when the initial concentration of GO is 80-100 mg.L^{-1}, increasing the concentration of GO can increase the adsorption point of CIT and enhance the electrostatic effect, which is reflected in the improvement of the adsorption rate of CIT to GO. When the GO concentration exceeds 100 mg.L^{-1}, the increase of the initial GO concentration will inhibit the electrostatic interaction between CIT and GO, resulting in the decline of the adsorption performance of CIT to GO. Fig. 9 shows the solution image of CIT after adsorption of GO under different

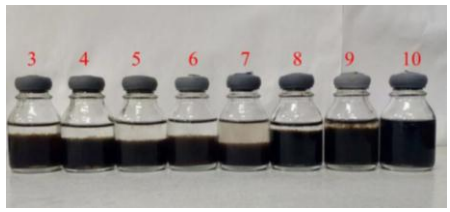

Fig. 5: Experimental picture of pH adsorbing GO to CIT at 7 days.

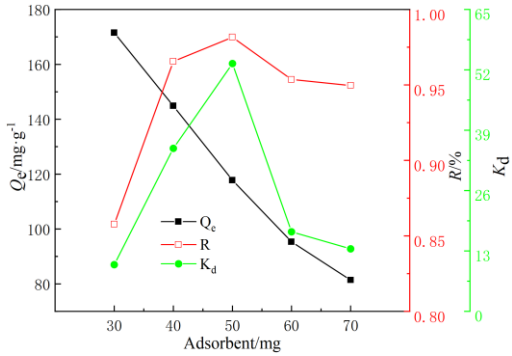

Fig. 6: Effect of CIT dosage on adsorption of GO.

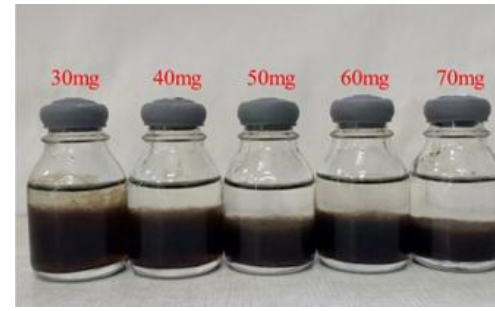

Fig. 7: Experimental pictures of the influence of CIT dosage on adsorption.

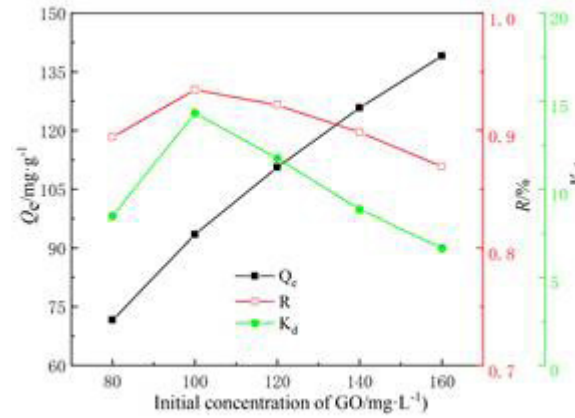

Fig. 8: Experimental pictures of the influence of CIT dosage on adsorption.

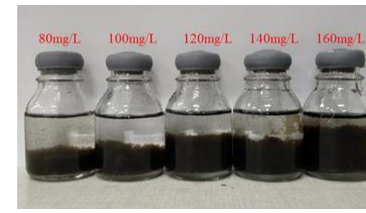

Fig. 9: Experimental pictures of the influence of CIT dosage on adsorption.

initial GO concentrations. It can be seen from Fig. 9 that CIT has high adsorption when the initial GO concentration is low. When the initial GO concentration is 100 mg.L^{-1}, the solution stratification is the clearest and the upper separation is the clearest.

Microscopic Characterization

To analyze the adsorption mechanism of CIT adsorbed GO, extracted the substance (CITGO) after CIT adsorbed GO, poured out the supernatant of the solution after CIT adsorbed GO, transferred the remaining suspension into a 10 mL polyethylene centrifuge tube with a pipette, and centrifuged it in a high-speed centrifuge (Shanghai Lichen Bangxi Instrument Technology Co., Ltd., L0-LX-HL210D) for solid-liquid two-phase separation, The centrifugation speed was set to 6000 rmp and the time was set to 2 minutes. After repeated centrifugation many times, it was put into a freeze dryer (Shanghai Yuming Instrument Co., Ltd., LGJ-10A) for freeze drying to obtain dry CITGO. The dried CITGO was characterized by SEM, TEM, EDS, FT-IR, XRD, XPS, and AFM to fully reveal the mechanism of CIT adsorbing GO from the changes of morphology, elements, crystals, and functional groups.

SEM and TEM

The SEM and TEM diagrams of GO, CIT, and CITGO are shown in Fig. 10. It can be clearly seen from Fig. 10 that GO is a typical two-dimensional material, characterized by smooth and relatively uniform flake structure (Fig. 10 (a)), while CIT in Fig. 10 (b) can see an obvious fast structure, which is formed by the formation of C-S-H gel after cement hydration reaction with iron tailings. In CITGO formed by CIT adsorbing GO, it can still be seen that it is similar to the CIT block structure in Fig. 10 (b), but its surface is smoother than that of CIT, which may be caused by the adsorption of GO with a smooth surface on CIT. this conjecture is proved in the TEM diagram of CITGO. From Fig. 10 (d), it can be seen that GO is like an open layer of tulle, and this layer of tulle in contact with CIT, is attached to CIT crystal particles (Fig. 10 (e)). Therefore, the observation of SEM and TEM test images showed that GO is adsorbed on the CIT surface. However, the surface of CITGO is not completely covered by GO. By comparing Fig. 10(b) and Fig. 10(c), Fig. 10(d), and Fig. 10(e), it can be found that some CIT is exposed, which reflects that the surface of CITGO may be a mixture of CIT and GO.

EDS, FT-IR and XRD

Fig. 11 shows EDS diagrams of GO, CIT, and CITGO, respectively. It can be seen from Fig. 11 that the main elements of CIT and CITGO are C, O, Mg, Al, Si, and Fe. In addition, the increase of the C element indicates the adsorption of GO on CIT, which indicates that CIT is the main surface of CITGO, which is consistent with the experimental structure of SEM and TEM. CITGO is a mixture of CIT and GO. To further verify this conjecture, GO, CIT and CITGO were characterized by FT-IR and XRD. The characterized test structure is shown in Fig. 12 and Fig. 13.

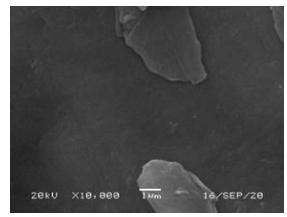

(a) GO

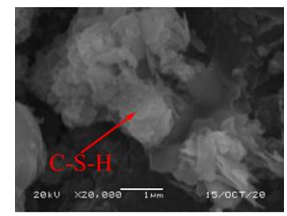

(b) CIT

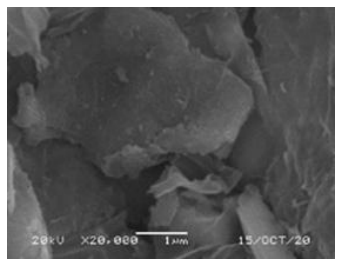

(c) CITGO

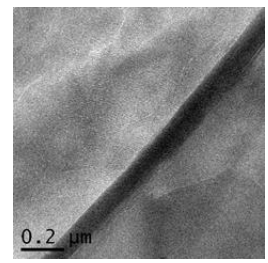

(d) GO

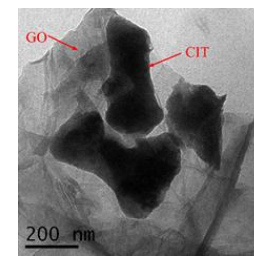

(e) CITGO

Fig. 10: SEM images of GO(a), CIT(b), and CITGO(c), TEM images of GO(d) and CITGO (e).

It can be seen from Fig. 12 that there is little difference between the spectra of GO, CIT, and CITGO, and the spectra between CIT and CITGO are the most similar. Among them, 1600 cm^{-1} ~ 1650 cm^{-1} is the characteristic absorption peak of C-S-H, and the wave peak is slightly stronger under acidic environmental conditions, so the higher the degree of polymerization is. It can be seen from Fig. 13 that the adsorption of GO under acidic conditions increases the oxygen-containing functional groups of CIT materials because the GO surface contains a large number of oxygen-containing functional groups. 3419 cm^{-1} is the stretching vibration absorption peak of the O-H bond, which is caused by the combined water in the CIT structure and the asymmetric stretching vibration of - OH in hydrated calcium silicate (Chen et al. 2019). In the XRD test results, there are also results similar to those of EDX and FT-IR. Among the spectra of GO, CIT, and CITGO, CIT and CITGO are the most similar, but there are also characteristic peaks of GO. Combined with the SEM and TEM test results, it shows that the surface of CITGO is a hybrid composition of CIT and GO, but the characteristics of CIT play a major role.

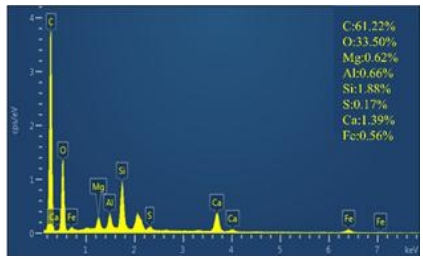

(a) CIT

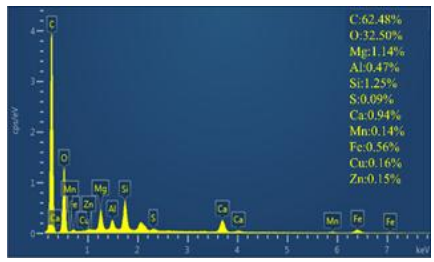

(b) CITGO

Fig. 11: EDS diagram of adsorption in different environments.

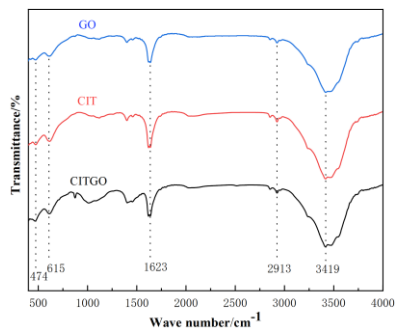

Fig. 12: FTIR diagram before and after adsorption in different environments.

Analysis of XPS and AFM

To provide more detailed information on CIT adsorption and GO adsorption mechanism, CIT and CITGO spectra before and after adsorption were analyzed by XPS, as shown in Fig. 14.

It can be found from Fig. 14 that O1s and C1s peaks appear at 530.97 eV and 283.97 eV, O1s and C1s peaks of CITGO are significantly stronger than GO, and N1s, Ca2p, and Si2p peaks also appear in crystal CITGO after adsorption. In addition, it can be observed that C1s are significantly enhanced after adsorption, indicating that CIT has a strong adsorption effect on GO. The high deconvolution of the C1s spectra of GO and CITGO before and after adsorption is shown in Fig. 14 (b). The C1s spectrum can be decomposed into four components at about 284.47 eV, 285.97 eV, and 289.32 eV, corresponding to C-C, C-O, and O-C=O structures respectively. When CIT adsorbs GO, the corresponding peak area increases greatly, indicating that some interactions have taken place between C-C, C-O, and O-C=O. Based on the above analysis, CIT can effectively adsorb GO. To some extent, SEM and TEM analyze the morphology of CITGO adsorbed by CIT on a two-dimensional scale. To further analyze the morphology of CITGO, the morphology of CITGO is analyzed on a three-dimensional scale by AFM, as shown in Fig. 15.

It can be seen from Fig. 15(a) that the maximum thickness of GO is about 1.19 nm, and from Fig. 15(b), the maximum thickness of the CITGO compound is about 17.51 nm, and the other peak is 16.81 nm. Compared with GO before adsorp-

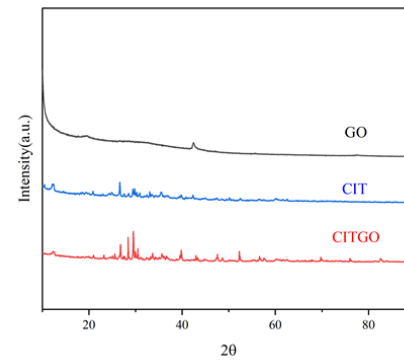

Fig. 13: Diffraction patterns before and after adsorption in different environments.

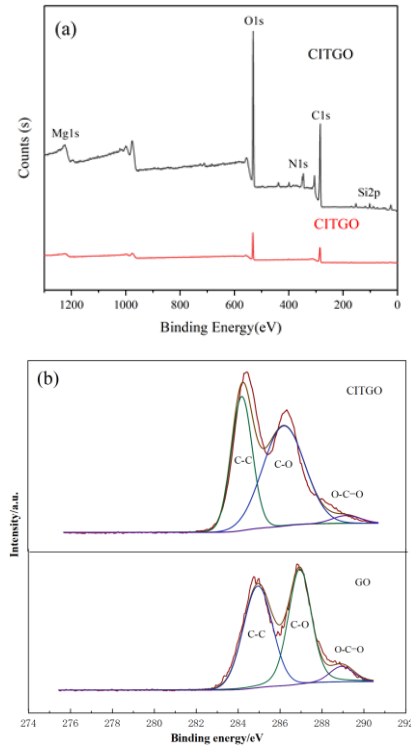

Fig. 14: XPS diagram before and after adsorption in different environments.

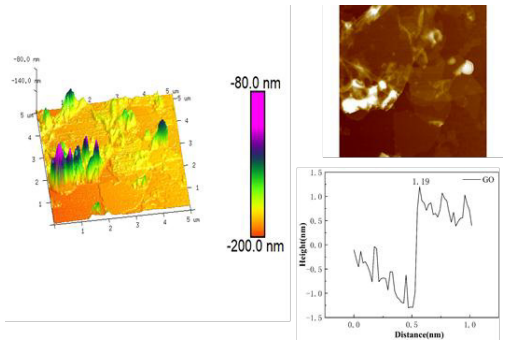

(a) GO

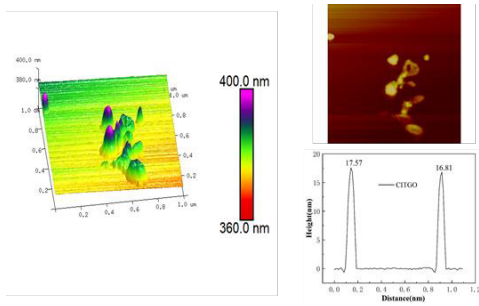

(b) CITGO

Fig. 15: AFM diagram before and after adsorption in different environments.

tion, the height of CITGO after CIT adsorbs GO increases significantly, and the surface becomes rougher, with different heights, showing double peaks. Combined with SEM, TEM, and two-dimensional images, the effective adsorption of CIT on GO is more fully explained.

CONCLUSION

CIT was obtained by strengthening iron tailings with cement, and the mechanical properties and GO adsorption capacity of CIT were studied. The main conclusions are as follows:

(1) Cement has a good reinforcement effect on iron tailings. The hydration reaction of cement is the main reason for strengthening iron tailings. The generated C-S-H can cement iron tailings, to improve the unconfined compressive strength of CIT, and this effect becomes more and more obvious with the increase of age because the longer the age, the more complete the hydration reaction of cement and the more C-S-H, which is reflected in the higher unconfined compressive strength of CIT.

(2) CIT at the age of 7 days had good adsorption performance for GO. When pH is 6, CIT content is 50 mg, and GO initial concentration is 100 mg.L^{-1}, CIT has the best adsorption effect on GO, and its adsorption rate is 93.5%. The adsorbed product CITGO was characterized by SEM, TEM, EDX, FT-IR, XRD, XPS, and AFM. It was found that GO was distributed on the surface of CIT, but the characteristics of CIT were significantly stronger than GO.

(3) With the increase of curing age, the zeta potential of CIT decreases, the bound water decreases, and the C-S-H products increase, resulting in asymmetric stretching vibration between the bound water and the O-H bond in C-S-H, weakening the relationship between the O-H bond and the oxygen-containing functional groups in GO, thus affecting the adsorption of CIT on GO.

REFERENCES

Chen, Y., Wu, Qi, Xiao, H., Xie, Y. and Wang, M. 2019. Formula optimization and mechanism of preparing geopolymers based on iron tailings and Metakaolin. Metal Mine, (04): 199-203.

Guan, S., Wu, F. and Zhao, B. 2014. MTT assay for detection of the cytotoxicity of graphene oxide. China Mod. Doc., 52(17): 18-20.

Jia, P. 2019. The Toxicological Mechanism of Graphene and Graphene Oxide. Chinese Academy of Sciences (Chongqing Institute of Green Intelligent Technology), Chongqing.

Li, B., Zhao, Z., Tang, B., Li, H., Cheng, H. and Ma, Z. 2018. Comprehensive utilization of iron tailings in China. IOP Conf. Series Earth Environ. Sci., 199(4): 042005.

Li, T., Zhang, C., Shen, D. and Yuan, Y. 2016. Research progress on biological toxicity of graphene and graphene oxide. J. Nanjing Univ. Nat. Sci., 52(02): 235-243.

Liu, F. and Wang, P. 2003. Modern water treatment methods and materials. China Environ. Sci. Press.

Luan, Z. and Tang, H. 1993. II. Adsorption of heavy metals by tailings sand. Environ. Chem., (05): 356-364.

Luo, H., Zhou, J., Zhang, Y., Hu, H., Huang, Z. and Shen, F. 2019. Preparation of graphene oxide and its adsorption properties for rhodamine B. New Chem. Mater., 47(01): 172-176.

Qiao, Y., An, J. and Ma, L. 2013. Single-cell array-based assay for in vitro genotoxicity study of nanomaterials. Anal. Chem., 85(8): 4107-4112.

Schinwald, A., Murphy, F.A., Jones, A., MacNee, W. and Donaldson, K. 2012. Graphene-based nanoplatelets: A new risk to the respiratory system as a consequence of their unusual aerodynamic properties. ACS Nano, 6(1): 736-746.

Sun, S., Sheng, Y., Sun, Q., Zheng, M., Li, Z. and Sun, X. 2017. Study on treatment of sludge thermal drying steam by activated carbon adsorption. Environ. Sci. Technol., 40(3): 650-658.

Tang, C., Chen, H., Ye, X. and Liu, M. 2016. Research progress on the removal of iron and manganese from groundwater by adsorption. J. Yangtze River Sci. Res. Instit., 33(6): 18-23.

Wang, J. 2017. Study of Graphene Oxide on Properties of Cement and Its Mechanism. Beijing University of Civil Engineering and Architecture, Beijing.

Yi, C., Tang, Q., Huang, X. and Qiu, X. 2012. Adsorption behavior of polycarboxylate superplasticizer on the surface of cement particles. Ciese J., (08): 2460-2468.

Yoon, Y., Park, W., Kyu, H., TaeMun, Y. and Dae, H. 2016. Comparative evaluation of magnetite–graphene oxide and magnetite-reduced graphene oxide composite for As (III) and As (V) removal. J. Hazard. Mater., 304: 196-204.

Zhao. Y., Hu, H. and Zhang, Qi. 2015. Treatment of chromium wastewater by steel slag. Appl. Chem. Ind., 044(8): 1496-1498, 1502.